Fluid Dynamics & Materials Processing
DOI:10.32604/fdmp.2020.09375
Article

Sliding Mode Control of Hydraulic Pressure in Electro-Hydraulic Brake System Based on the Linearization of Higher-Order Model

Qiping Chen*, Haoyu Sun, Ning Wang, Zhi Niu and Rui Wan

Key Laboratory of Conveyance and Equipment Ministry of Education, East China Jiaotong University, Nanchang, 330013, China
*Corresponding Author: Qiping Chen. Email: qiping3846758@163.com
Received: 08 December 2019; Accepted: 16 March 2020

Abstract: The possibility to enhance the stability and robustness of electro-hydraulic brake (EHB) systems is considered a subject of great importance in the automotive field. In such a context, the present study focuses on an actuator with a four-way sliding valve and a hydraulic cylinder. A 4-order nonlinear mathematical model is introduced accordingly. Through the linearization of the feedback law of the high order EHB model, a sliding mode control method is proposed for the hydraulic pressure. The hydraulic pressure tracking controls are simulated and analyzed by MATLAB/Simulink soft considering separately different conditions, i.e., a sine wave, a square wave and a square wave with superimposed sine disturbance. The results show that the proposed strategy can track the target within 0.25 s, and the mean observed error is less than 1.2 bar. Moreover, with such a strategy, faster response and less overshoot are possible, which should be regarded as significant advantages.

Keywords: EHB; hydraulic pressure; feedback linearization; sliding mode control

1 Introduction

1.1 Research Background

Over the recent years, the development trend of electrification, networking, intelligence, and sharing of automotive has been actively responded and supported by variable automotive manufacturers and suppliers home and abroad [1]. Many advanced solutions for conventional automotive parts and relevant technics researches emerged, and the EHB is one of them. The electro-hydraulic brake system, with EHB for short, is a kind of brake system, which can replace the vacuum booster absolutely and improve the control effect to the brake request better. Apart from that, the EHB can also generate the expected brake force within the range required by regulations, decrease the response time and be easy to match with brake energy recycling function. But, the real running condition of automotive is very adverse for hydraulic pressure control, and the strong real-time transience would result in distortion to real-time hydraulic control at variable levels and the universal nonlinear factors would result in the physical model hard to construct and meanwhile the control strategy hard to take effect [2]. Therefore, with the order that EHB would work reliably and stably, the feasibility and validity research about resolving target pressure and controlling real-time pressure has to be implemented.

1.2 Research Status

A large number of studies about the EHB system have been carried out at home and abroad. Yu et al. [3] at Tongji University designed an I-EHB, and analyzed its nonlinear factors with Stribeck friction model-based, and designed an anti-integral saturation control measure, but didn't take the fluid nonlinear factor into account. He et al. [4] at Tsinghua University designed a double closed-loop strategy of slip rate and brake torque with I-EHB model and 7-DOF vehicle model-based but didn't take the fluid nonlinear factor into account. Chen et al. [5] at Jilin University proposed a hybrid by-wire brake system with EHB in the front axle and EMB in the rear axle but didn't take the nonlinear factor into account. Chen et al. [6] at Jiangsu University designed a tandem electro-hydraulic hybrid brake structure, a brake distribution strategy, and a logic threshold-based pressure control strategy, but didn't take the nonlinear factor into account. Wang et al. [7] developed a robust wheel slip controller for in-wheel-motors-driven electric vehicles. Raffone [8] proposed an algebraic mathematical model with motor on caliper aimed and designed a robust EPB control strategy. Jegadeeshwaran et al. [9] proposed an on-line condition monitoring by using a machine learning approach and acquired the vibration signals for both good as well as faulty conditions of brakes. Ruderman et al. [10] proposes a sensorless estimation of external load forces with the nonlinearity and dependency of sensor aimed at when observing the load in standard hydraulic actuators. Cheng et al. [11] proposed a sliding mode control strategy based high-precision hydraulic pressure feedback modulation including an open-loop load pressure control and validated a HIL test rig. Xing et al. [12] developed an integrated time series model (TSM) based on multivariate deep recurrent neural networks (RNN) with long short-term memory (LSTM) units and then constructed a real-time multivariate LSTM-RNN model for the dynamic estimation of the brake pressure of EVs. Chen et al. [13] proposed and designed a sliding mode control method for the master cylinder hydraulic pressure and assessed the nonlinear characteristics of the system involved, but lacked the application of higher-order model and relevant nonlinear theory in designing the control strategy.

1.3 Scientific and Engineering Contributions

The research for methods or theories of hydraulic pressure control to the electro-hydraulic brake system is one of the urgencies in the process of developing the electric vehicle. Based on the requirements of the stability and robustness of the electro-hydraulic brake (EHB) system, according to the feedback linearization theory, the 4-order nonlinear mathematical model of an actuator with a four-way sliding valve and a cylinder is established. Then, based on the model, a sliding mode control method is proposed and designed. After several simulations, the results show that the proposed strategy can track the target within 0.25 s, and the mean observed error is less than 1.2 bar. Moreover, with such a strategy, faster response and less overshoot are possible.

1.4 Research Working

Based on the analysis of relevant researches home and abroad, a 4-order nonlinear mathematical model is established according to the feedback linearization theory. Then, a sliding mode control method based on the model is designed, aiming at the nonlinear higher-order EHB model proposed.

2 Actuator Design and Model Establishment

At the view of the structure, the EHB discards the vacuum booster, which depends on the engine to work and consists of electromechanical and hydraulic subsystems. Of them, the electromechanical subsystem consists of ECU, motor part, sensor part, and mechanics powertrain part; the hydraulic subsystem consists of a master cylinder, pipeline, electromagnet valves, and wheel cylinder. Due to the necessity to research, the actuator in EHB assembled by a four-way sliding valve and a wheel-cylinder is used to the research object.

Because of the advantages of small space to occupy, simple structure, low cost, and better loading ability of the asymmetric cylinder [14], so the wheel-cylinder is chosen to be the hydraulic actuator. Besides, it is used to transform the hydraulic energy in wheel-cylinder into mechanical energy to generate brake torque. The hydraulic subsystem controlled by the sliding valve its structure is shown in Fig. 1.

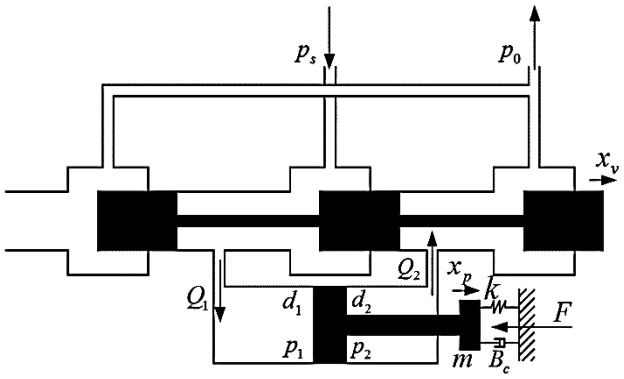

Figure 1: Valve control EHB physical model

As shown in Fig. 1, the adopted asymmetric cylinder is an ideal-zero-opened four-way sliding valve, which means that its four orifices are symmetrical and matched. The flow in its throttle is turbulent, and the fluid compressibility in it is ignored, the spool of it can move and fluid can flow in instance, the pressure in each one chamber is equal anywhere, and the supply pressure p_s is constant while the return pressure p_0 is zero; the pipelines are all short and thick; the influence of fluid mass and the dynamic effect of pipeline are ignored; the fluid temperature and volume modulus are considered as constant in the simulation duration; the external leakage in wheel-cylinder is laminar flow [14]; the direction that the piston push toward is regarded as the forward kinematics.

The flow equation of the sliding valve is shown in Eqs. (1) and (2).

$$Q_1 = K_d x_v \sqrt{\left[\frac{(1+\mathrm{sgn}(x_v))p_s}{2} + \frac{(-1+\mathrm{sgn}(x_v))p_0}{2} - \mathrm{sgn}(x_v)p_1\right]} \tag{1}$$

$$Q_2 = K_d x_v \sqrt{\left[\frac{(1-\mathrm{sgn}(x_v))p_s}{2} + \frac{(-1-\mathrm{sgn}(x_v))p_0}{2} + \mathrm{sgn}(x_v)p_2\right]} \tag{2}$$

where K_d is presented as $K_d = C_d\omega\sqrt{\frac{2}{\rho}}$.

And the flow continuity equations of the cylinder are shown in Eqs. (3) and (4).

$$Q_1 = A_1\dot{x}_p + C_{ic}(p_1 - p_2) + C_{ec}p_1 + \frac{V_{g1} + A_1L_0 + A_1x_p}{\beta_e}\dot{p}_1 \tag{3}$$

$$Q_2 = A_2\dot{x}_p + C_{ic}(p_1 - p_2) - C_{ec}p_2 - \frac{V_{g2} + A_2(L - L_0) - A_2x_p}{\beta_e}\dot{p}_2 \tag{4}$$

where, ω is the area gradient at sliding valve port when the sliding valve port with variable flowing resistance is full circumference then $\omega = \pi \cdot d$, C_{ic} is the internal flow leakage coefficient, L is the total piston travel, L_0 is the initial piston position, x_p is the piston motion displacement, β_e is the fluid volume modulus, V_{g1} is the

inlet pipeline volume from sliding valve to wheel-cylinder, V_{g2} is the outlet pipeline volume from wheel-cylinder to sliding valve.

The equation of force is shown in Eq. (5).

$$A_1 p_1 - A_2 p_2 = m\ddot{x}_p + B_c\dot{x}_p + kx_p + F \tag{5}$$

In Eq. (5), the A_1, $A_2$are presented in Eqs. (6) and (7).

$$A_1 = \frac{\pi {d_1}^2}{4} \tag{6}$$

$$A_2 = \frac{\pi\left({d_1}^2 - {d_2}^2\right)}{4} \tag{7}$$

where, m is the total mass of rod and piston in wheel-cylinder; B_c is the equivalent fluid damping coefficient; k is the equivalent contacting stiffness between the brake disc and brake slipper.

And as the sliding valve is also a twin flapper-nozzle electro-hydraulic servo sliding valve, so its dynamic model can be presented as a proportional component [15] as shown in Eq. (8).

$$x_v = K_r K_{axv} f_e \tag{8}$$

In Eq. (8), the f_e is presented in Eq. (9).

$$f_e = p_e A_1 - p_2 A_2 \tag{9}$$

where, K_{axv} is the gain of the servo valve; p_e is the expected pressure in brake wheel-cylinder; K_r is the gain of the hydraulic pressure sensor.

3 Feedback Linearization to Nonlinear Model

According to the established nonlinear mathematical model, the rod displacement x_p, rod velocity $\dot{x}_p$, hydraulic pressure p_1 in the chamber without the rod of wheel-cylinder, and hydraulic pressure p_2 in the chamber with the rod of wheel-cylinder are chosen to be the system state variable, which is shown in Eq. (10).

$$x = [x_1 \quad x_2 \quad x_3 \quad x_4]^T = [x_p \quad \dot{x}_p \quad p_1 \quad p_2]^T \tag{10}$$

The f_e is the input variable and presented in Eq. (11). And the nonlinear state equation is presented in Eq. (12).

$$u = f_e \tag{11}$$

$$\begin{cases} \dot{x} = f(x) + g(x)u \\ y = h(x) = A_1 x_3 - A_2 x_4 \end{cases} \tag{12}$$

The state variables $\dot{x}_1$, $\dot{x}_2$, $\dot{x}_3$, and $\dot{x}_4$ are shown in Eqs. (13)–(16).

$$\dot{x}_1 = \dot{x}_p = x_2 \tag{13}$$

$$\dot{x}_2 = \ddot{x}_p = \frac{-kx_1 - B_c x_2 + A_1 x_3 - A_2 x_4 - F}{m} \tag{14}$$

$$\dot{x}_3 = \dot{p}_1 = \frac{\beta_e[Q_1 - A_1 x_2 - (C_{ic} + C_{ec})x_3 + C_{ic}x_4]}{V_{g1} + A_1(L_0 + x_p)} \tag{15}$$

$$\dot{x}_4 = \dot{p}_2 = -\frac{\beta_e[Q_2 - A_2 x_2 - C_{ic}x_3 + (C_{ic} + C_{ec})x_4]}{V_{g2} + A_2(L - L_0 - x_p)} \tag{16}$$

The argumentation above can be concluded in Eqs. (17)–(24).

$$f(x) = [f_1 \;\; f_2 \;\; f_3 \;\; f_4]^T \tag{17}$$

$$g(x) = [0 \;\; 0 \;\; g_3 \;\; g_4]^T \tag{18}$$

$$f_1 = x_2 \tag{19}$$

$$f_2 = \frac{-kx_1 - B_c x_2 + A_1 x_3 - A_2 x_4 - F}{m} \tag{20}$$

$$f_3 = \frac{\beta_e[-A_1 x_2 - (C_{ic} + C_{ec})x_3 + C_{ic}x_4]}{V_{g1} + A_1(L_0 + x_p)} \tag{21}$$

$$f_4 = -\frac{\beta_e[-A_2 x_2 - C_{ic}x_3 + (C_{ic} + C_{ec})x_4]}{V_{g2} + A_2(L - L_0 - x_p)} \tag{22}$$

$$g_3 = \frac{\beta_e K_r K_{axv} K_d}{V_{g1} + A_1 L_0 + A_1 x_1} \sqrt{\left[\frac{(1 + \mathrm{sgn}(u))p_s}{2} + \frac{(-1 + \mathrm{sgn}(u))p_0}{2} - \mathrm{sgn}(u)p_1\right]} \tag{23}$$

$$g_4 = -\frac{\beta_e K_r K_{axv} K_d}{V_{g2} + A_2(L - L_0) - A_2 x_1} \sqrt{\frac{2}{\rho}\left[\frac{(1 - \mathrm{sgn}(u))p_s}{2} + \frac{(-1 - \mathrm{sgn}(u))p_0}{2} + \mathrm{sgn}(u)p_2\right]} \tag{24}$$

According to the definition of Lie Derivative [16], the results shown below can be calculated.

$$L^0{}_f h(x) = A_1 x_3 - A_2 x_4 \tag{25}$$

$$L_g L^0{}_f h(x) = A_1 g_3 - A_2 g_4 \tag{26}$$

$$L_f h(x) = A_1 f_3 - A_2 f_4 \tag{27}$$

According to the definition of relative order [16], the relative order of this system is 1. And due to the system is a four-order system, an internal dynamic subsystem exists. In accordance with the theory of feedback linearization in the nonlinear system, a transformation should be implemented on that subsystem [6], and then a linear state equation is obtained, presented in Eq. (28).

$$\begin{cases} \dot{z} = v \\ y = z \end{cases} \tag{28}$$

In Eq. (28), the z is a one order vector, and the transformation relation of state variable can be presented in Eq. (29).

$$\begin{cases} z = h(x) = A_1 x_3 - A_2 x_4 \\ y = z \end{cases} \tag{29}$$

In Eq. (28), the transformation relation of the input variable v can be presented in Eq. (30).

$$v = \alpha(x) + \beta(x)u \tag{30}$$

The α and β are presented in Eqs. (31) and (32).

$$\alpha(x) = L_f h(x) \tag{31}$$

$$\beta(x) = L_g L^0{}_f h(x) \tag{32}$$

In Eq. (33), the input variable u in nonlinear state space can be calculated from the input variable v in linear state space by inverse transformation [16].

$$u = \frac{v - \alpha(x)}{\beta(x)} \tag{33}$$

4 Sliding Mode Controller Design

Due to the limited condition to observe and measure, the precise nonlinear mathematical model is hard to obtain when designing the feedback linearization control law. As to the servo wheel-cylinder controlled by the sliding valve adopted in EHB in this paper, the variation of the load, the fluid viscosity, the supply pressure, and the wear condition on some contact area would affect the tracking control of hydraulic pressure.

So, it is necessary to introduce a robust control algorithm to ensure the robustness to the parameter variation and external disturbance [17] for the system transformed by feedback linearization.

First, the tracking pressure error [18] is defined as Eq. (34).

$$e = z_e - z \tag{34}$$

In the Eq. (34), the z_e is the expected pressure in wheel-cylinder of the system transformed by feedback linearization. Due to the relative order of the system transformed by feedback linearization which is indicated to be 1 [16]. So, the sliding mode surface can be designed as Eq. (35).

$$s = e \tag{35}$$

Then, the equivalent control v_{eq} is settled as Eq. (36).

$$\dot{s} = \dot{e} = \dot{z}_e - \dot{z} \tag{36}$$

When $\dot{s} = 0$, then v_{eq} equals to $\dot{z}_e$ obviously.

It is required that $s\dot{s} < 0$ is permanently met to ensure the sliding mode exists [18]. So, the switching control v_{sw} is settled as Eq. (37).

$$v_{sw} = -\kappa \cdot sgn(s) \tag{37}$$

In the Eq. (37), the κ is the gain of the switching control. Then, the output of the designed controller can be stated as Eq. (38).

$$v = v_{eq} + v_{sw} = \dot{z}_e - \kappa \cdot sgn(s) \tag{38}$$

In order to verify the stability of the control algorithm, the *Lyapunov* [11] function is settled in Eq. (39).

$$V = \frac{1}{2}s^2 \tag{39}$$

Additionally, the relative process can be calculated according to Eqs. (34)–(39) and shown in Eqs. (40)–(44).

$$\dot{V} = s\dot{s} \tag{40}$$

$$\dot{V} = s(\dot{z}_e - \dot{z}) \tag{41}$$

$$\dot{V} = s[\dot{z}_e - \kappa \cdot sgn(s) - \dot{z}_e] \tag{42}$$

$$\dot{V} = s[-\kappa \cdot sgn(s)] \tag{43}$$

$$\dot{V} = -\kappa \cdot |s| \leq 0 \tag{44}$$

Therefore, it is indicated that the control system in the linear space after transformation is stable. But, due to the chattering with which the sign function would bring to the system, so, it is replaced by the boundary layer function to weaken the chattering [20]. The boundary layer function is demonstrated as Eq. (45).

$$sat\left(\frac{s}{\Phi}\right) = \begin{cases} sgn\left(\frac{s}{\Phi}\right) & \left(\left|\frac{s}{\Phi}\right| > 1\right) \\ \frac{s}{\Phi}\left(\left|\frac{s}{\Phi}\right| < 1\right) & \left(\left|\frac{s}{\Phi}\right| < 1\right) \end{cases} \tag{45}$$

In Eq. (45), the Φ is the thickness of the boundary layer.

According to Eqs. (32)–(45), the sliding mode control law u can be calculated and shown as Eq. (46).

$$u = \frac{\dot{z}_e - \kappa \cdot sat\left(\frac{s}{\Phi}\right) - L_f h(x)}{L_g L^0{}_f h(x)} \tag{46}$$

5 Simulation and Verification

According to the feedback linearization theory, and the linearization to the model of cylinder controlled by servo sliding valve in the EHB, and the sliding mode control algorithm designed in this paper, a simulation model is established in MATLAB/Simulink. The model is shown in Fig. 2 below. As shown in Fig. 3 below, it illustrates the control logic designed in this paper.

Then, the tracking simulation verifications to the pressure signal in the sine wave, square wave, and the square wave with sine wave disturbance mixed, are implemented. The parameters used in the simulation are listed in Tab. 1.

5.1 Simulation and Verification under Sine Wave Signal

First, the pressure signal in the sine wave with mean value 5 MPa, amplitude 10 MPa, and frequency 0.25 Hz is adopted to the tracking simulation for 4 s. And the simulation result is shown in Figs. 4 and 5 below.

It can be inferred from Figs. 4 and 5, that the mean tracking error to the pressure signal in the sine wave is −0.03931 MPa, and phase delay is acceptable under the sliding mode control algorithm. In the duration of the simulation, the pressure responded to the target pressure signal starts keeping stable tracking error at the time of 0.25 s.

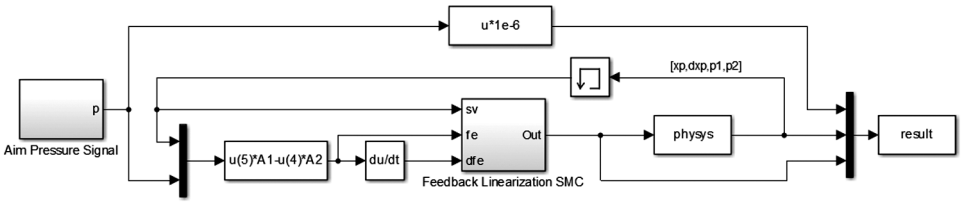

Figure 2: MATLAB/Simulink model

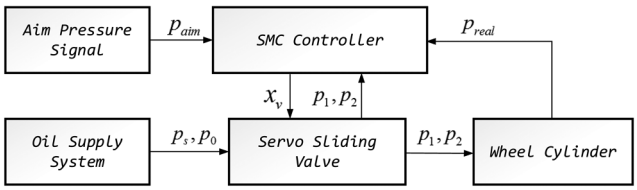

Figure 3: Control logic diagram

Table 1: Simulation parameters

Parameter	Value	Unit	Parameter	Value	Unit
ρ	850	kg/m^3	C_{ic}	4.5e-13	m N/s
β_e	1.7e4	N/m^3	C_{ec}	4.5e-13	m N/s
m	0.6	Kg	d_1	0.07	m
L_0	2e-3	m	d_2	0.032	m
L	0.12	m	p_0	0	Pa
B_c	1.1e4	N(m/s)	p_s	1.2e7	Pa
k	3.37e7	N/m	φ	4.15e4	–
ω	1.57e-2	–	κ	2.155e13	–
C_d	0.67	–	K_{axv}	0.8	–
$V_{gi(i=1,2)}$	2e-5	m^3	K_r	1e-5	–

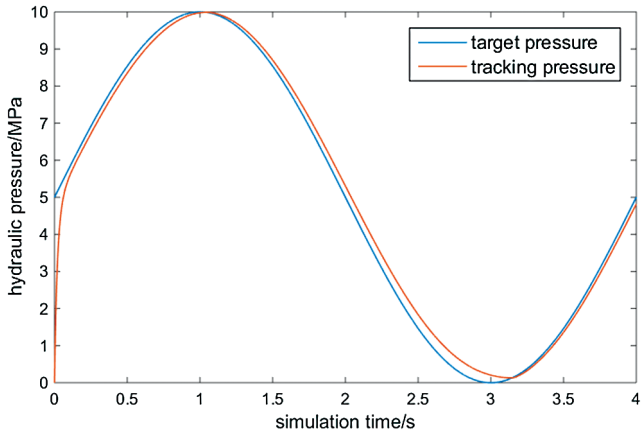

Figure 4: Tracking simulation result of the pressure signal in the sine wave

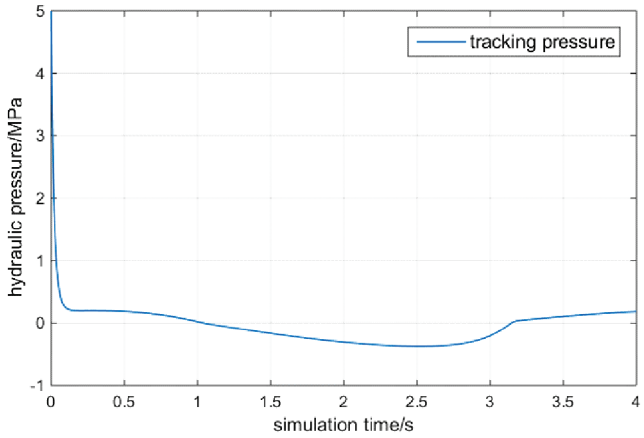

Figure 5: Tracking simulation error of the pressure signal in the sine wave

5.2 Simulation and Verification under Square Wave Signal

Second, the pressure signal in the square wave with amplitude 10 MPa, and frequency 0.25 Hz is adopted to the tracking simulation for 4 s. And the simulation result is showed in Figs. 6 and 7.

It can be inferred from Figs. 6 and 7, that the mean tracking error to the pressure signal in the square wave is −0.0801 MPa under the sliding mode control algorithm. In the duration of the simulation, the pressure responded to the target pressure signal starts keeping stable tracking error at the time of 0.1 s.

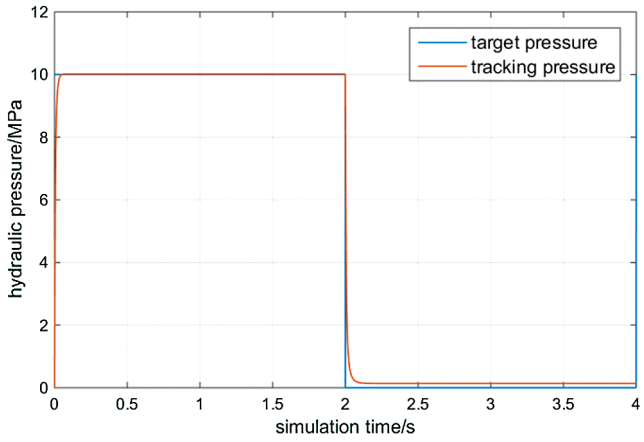

Figure 6: Tracking simulation result of the pressure signal in the square wave

5.3 Simulation and Verification under Superimposed Sine-Square Wave Signal

Last, to validate the stability of the robust control algorithm designed in this paper, the pressure signal in the square wave with superimposed sine disturbance is adopted to the tracking simulation for 4 s. This pressure signal contains the square wave with amplitude 10 MPa, and frequency 0.25 Hz and the sine disturbance with mean value 0 MPa, amplitude 0.5 MPa, and frequency 0.25 Hz. The simulation result is shown in Figs. 8 and 9.

It can be inferred from Figs. 8 and 9, that the mean tracking error to the pressure signal in the square wave with superimposed sine disturbance is −0.1186 MPa under the sliding mode control algorithm. In the duration of the simulation, the pressure responses to the target pressure signal and starts keeping

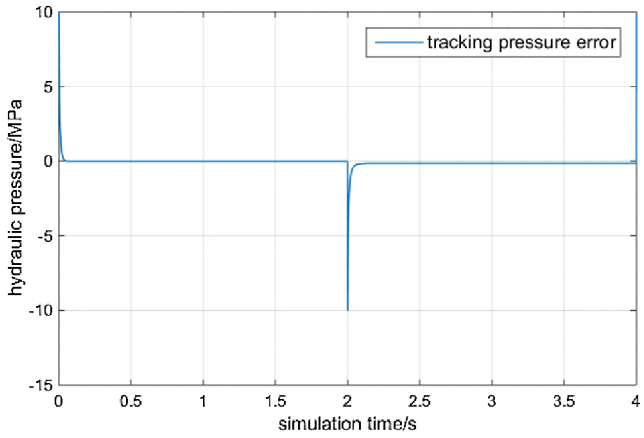

Figure 7: Tracking simulation error of the pressure signal in the square wave

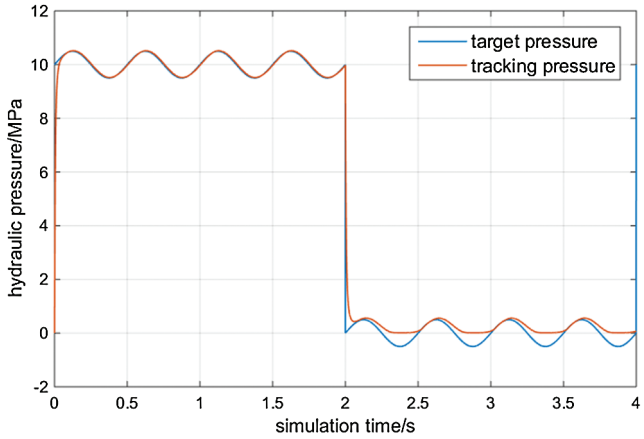

Figure 8: Tracking simulation result of the pressure signal in the square wave with superimposed sine disturbance

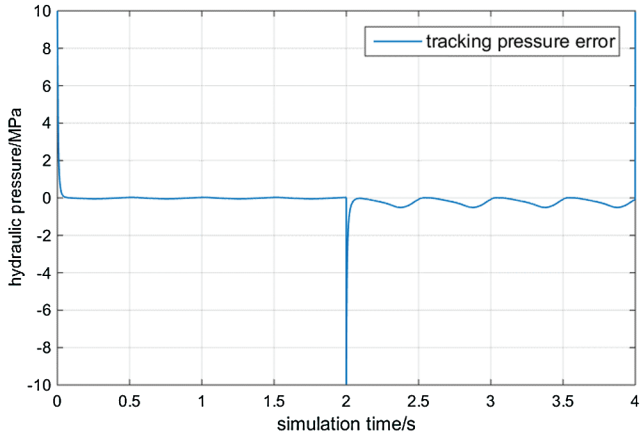

Figure 9: Tracking simulation error of the pressure signal in the square wave with superimposed sine disturbance

stable tracking error at the time of 0.1 s, and the tracking error is more stable in the high target pressure signal phase than in the low target pressure signal phase.

6 Conclusions

The brake wheel-cylinder controlled by a servo sliding valve, which is consisted of the four-way sliding valve and cylinder with ideal feature, is adopted as the research object. Then, with the requirementof the response efficiency and robustness of EHB aimed, the 4-order mathematical model of brake wheel-cylinder controlled by servo sliding valve is settled. After that, the feedback linearization theory is introduced to implement a linear transformation and a sliding mode control of hydraulic pressure based feedback linearization of high order EHB model is proposed. Last, some simulations are implemented in MATLAB/Simulink and the simulation results are analyzed.

By implementing the research stated above, some conclusions are obtained and stated below.

1. By applying the feedback linearization theory, the nonlinearity of the proposed valve control hydraulic wheel-cylinder is transformed into approximate linearity when designing the SMC controller, which proves correct and characterizes the novelty of the work in this paper.
2. The response characteristic, tracking effect and the phase delay are well limited in an acceptable section for the tracking simulations, under the pressure signal in the sine wave, in the square wave, and in the square wave with sine wave disturbance mixed. And they indicate that the strategy of sliding mode control of hydraulic pressure based feedback linearization of high order EHB model proposed in this paper can track the target within 0.25 s, and the mean observed error is less than 1.2 bar. Therefore, this research shows that the strategy designed has the advantages of faster response and less overshoot, which can be considered as a theory reference for further hydraulic pressure control research of EHB.

In the near future, there are some works left to be researched further, which are stated below.

1. The research physical model needs to be expanded into an integrated system. Therefore, at least, a detailed oil supply system and a specific actuator for the spool of servo sliding valve should be designed and verified, and which then should be added to the current model.
2. Some other typical aim pressure signals and relevant requirements of regulations should be added in the part of simulation and verification to prove the control method flexible and its robustness in the further.

Acknowledgement: The authors would like to thank anonymous reviewers for their helpful comments and suggestions to improve the manuscript.

Funding Statement: This work was supported by the National Natural Science Foundation of China [grant number 51565011], and the Foundation of Educational Department of Jiangxi Province [grant number GJJ180302].

Conflicts of Interest: The authors declare that they have no conflicts of interest to report regarding the present study.

References

1. Editorial Department of China Journal of Highway and Transport. (2017). Review on China's automotive engineering research progress. *China Journal of Highway and Transport, 20(166),* 5–201.
2. Lv, C., Hu, X., Sangiovanni-Vincentelli, A., Li, Y., Martinez, C. M. et al. (2019). Driving-style-based codesign optimization of an automated electric vehicle: a cyber-physical system approach. *IEEE Transactions on Industrial Electronics, 66(4),* 2965–2975. DOI 10.1109/TIE.2018.2850031.
3. Yu, Z., Han, W., Xiong, L. (2017). Variable structure control for hydraulic pressure in integrated-electro-hydraulic brake system. *Automotive Engineering, 39(1),* 52–60.

4. He, X. K., Ji, X. W., Yang, K. M., Wu, J. (2018). Tire slip control based on integrated-electro-hydraulic braking system. *Journal of Jilin University (Engineering and Technology Edition), 48(2),* 364–372.
5. Chen, Z. C., Wu, J., Zhao, J., He, R. (2018). Control strategy for accurate adjustment of braking force in hybrid brake by wire system. *Automotive Engineering, 40(4),* 457–464.
6. Chen, L., Sun, D. H., Pan, C. F. (2018). Tandem type electro-hydraulic compound braking system and hydraulic control. *Journal of Henan University of Science and Technology (Natural Science), 39(5),* 18–23.
7. Wang, B., Huang, X., Wang, J., Guo, X., Zhu, X. (2015). A robust wheel slip ratio control design combining hydraulic and regenerative braking systems for in-wheel-motors-driven electric vehicles. *Journal of the Franklin Institution, 352(2),* 577–602. DOI 10.1016/j.jfranklin.2014.06.004.
8. Raffone, E. (2017). An electric parking brake motor-on-caliper actuator model for robust drive a way control design. *IFAC-Papers on Line, 50(1),* 980–986. DOI 10.1016/j.ifacol.2017.08.177.
9. Jegadeeshwaran, R., Sugumaran, V. (2015). Fault diagnosis of automobile hydraulic brake system using statistical features and support vector machines. *Mechanical Systems and Signal Processing, 52,* 436–446. DOI 10.1016/j.ymssp.2014.08.007.
10. Ruderman, M., Fridman, L., Pasolli, P. (2019). Virtual sensing of load forces in hydraulic actuators using second- and higher-order sliding modes. *Control Engineering Practice, 92,* 104151. DOI 10.1016/j.conengprac.2019.104151.
11. Lv, C., Wang, H., Cao, D. P. (2017). High-precision hydraulic pressure control based on linear pressure-drop modulation in valve critical equilibrium state. *IEEE Transactions on Industrial Electronics, 64(10),* 7984–7993. DOI 10.1109/TIE.2017.2694414.
12. Yang, X., Lv, C. (2019). Dynamic state estimation for the advanced brake system of electric vehicles by using deep recurrent neural networks. *IEEE Transactions on Industrial Electronics*. DOI 10.1109/TIE.2019.2952807.
13. Chen, Q., Liu, Y., Zeng, L., Xiao, Q., Zhou, C. et al. (2018). On the control of the master cylinder hydraulic pressure for electro-hydraulic brake (EHB) systems with the sliding mode design methodology. *Fluid Dynamics & Materials Processing, 14(4),* 281–291. DOI 10.32604/fdmp.2018.03721.
14. Song, Z. A., Cao, L. M., Huang, J. (2012). *MATLAB/Simulink and hydraulic control system simulation*. Beijing: National Defense Industry Press.
15. Xiong, L., Pan, G. L., Shu, Q., Xu, G. D., Yu, Y. et al. (2019). Pressure control of integrated electronic hydraulic brake system. *Mechatronics, 25(3),* 10–19.
16. Hassan, K. K., Zhu, Y. S., Dong, H., Li, Z. Z. (2005). *Nonlinear system*. Beijing: Publishing House of Electronics Industry.
17. Shang Guan, W. B., Liang, S. Q., Liang, K. H., Tang, W. (2019). Modeling and pressure control of integrated electro-hydraulic brake system. *Transactions of Beijing Institute of Technology, 39(4),* 413–418.
18. Li, N., Ning, X., Wang, Q., Li, J. (2017). Hydraulic regenerative braking system studies based on a nonlinear dynamic model of a full vehicle. *Journal of Mechanical Science and Technology, 31(6),* 2691–2699. DOI 10.1007/s12206-017-0512-7.
19. Liu, J. K. (2005). *The MATLAB simulation of sliding mode variable structure control*. Beijing: Tsinghua University Press.
20. Tan, Z. H., Chen, Z. F., Pei, X. F., Guo, X. X., Pei, S. H. (2016). Development of integrated electro-hydraulic braking system and its ABS application. *International Journal of Precision Engineering and Manufacturing, 17(3),* 337–346. DOI 10.1007/s12541-016-0042-8.